京都大学防災研究所年報 第 54 号 B 平成 23 年 6 月
Annuals of Disas. Prev. Res. Inst., Kyoto Univ., No. 54 B, 2011

Interactive Behavior of the Pleistocene Reclaimed Foundations due to the Construction of the Adjacent Reclamation

Byung-Gon JEON* and Mamoru MIMURA

* Graduate School of Engineering, Kyoto University

Synopsis

A series of elasto-viscoplastic finite element analyses is performed to assess the interactive behavior of the Pleistocene foundations due to the construction of the adjacent two reclaimed islands of Kansai International airport in Osaka Bay. The concept of "mass permeability" is introduced to model the actual process of dissipation of excess pore water pressure in the field. The mechanism for the propagation of excess pore water pressure due to the construction of the adjacent reclamation is also discussed through the numerical analyses. The modeling of compressibility for the quasi-overconsolidated Pleistocene clays is adopted because high compressibility induced by the highly developed structure of the Pleistocene clays causes the large and long-term settlement. The present numerical analyses are found to describe the large and long-term settlement together with the insufficient dissipation and the propagation of excess pore water pressure due to the construction of the adjacent reclamation in the Pleistocene clay and sand gravel layers that actually has taken place in the field. The calculated performance is validated by comparing with the measured results.

Keywords: elasto-viscoplastic finite element analysis, mass permeability, quasi-overconsolidated, interactive behavior

1. Introduction

The outstanding development of coastal areas has recently been accomplished in Japan. Kansai International Airport (KIX) was constructed in Osaka Bay as two man-made reclaimed islands to minimize noise and pollution in residential areas as well as to meet the increasing demand for air transportation. The 1st phase island was constructed 5km offshore from the coastal line and the adjacent 2nd phase island was constructed after completion of the 1st reclamation. A large-scale offshore reclamation in Osaka Bay is accompanied with large and rapid settlement of deep Pleistocene clay deposits (Mimura et al., 2003). The seabed deposits of Osaka Bay have been formed due to the soil supply from the rivers on the sinking base (Kobayashi et al., 2001). Although it is common that the clay deposits formed under this environment should be normally consolidated, the Pleistocene clays in Osaka Bay exhibit slight overconsolidation with OCR of 1.2 to 1.6 in average. This seeming overconsolidation is thought not to arise from the mechanical reason but to be subjected to the effect of diagenesis, such as aging effect and/or development of cementation among clay particles. In the sense, the Pleistocene clays deposited in Osaka Bay is so-called "quasi-overconsolidated clays" without definite mechanical overconsolidation history and can also be regarded as "normally consolidated aged clays" with seeming overconsolidation. Akai and Sano

(1981) called those clays as "quasi-overconsolidated clays" by distinguishing them from the mechanical overconsolidated clays. On the basis of these findings, Mimura and Jang (2004) proposed a new concept of compression in which viscoplastic behavior is assumed to occur even in the quasi-overconsolidated region less than pc for the Pleistocene clays in Osaka Bay.

On the basis of the data from elastic wave exploration and in-site boring logs, Ito et al. (2001) summarized that the Pleistocene sand gravel deposits are not always distributed uniformly in thickness, continuously and that not a small amount of fine contents is included in them. The most serious problem originating from these sand gravel deposits is "permeability" that controls the rate of consolidation of sandwiched Pleistocene clays because it does not necessarily follow that the net values of the coefficient of permeability based on laboratory experiments function as representatives for such non-uniform sand gravel layers with occasional horizontal discontinuity and/or variation of thickness. Therefore, the concept of "mass permeability" for the Pleistocene sand gravel layers is also introduced in this paper. The authors considered this practical permeability as "mass permeability" that effectively controls the process of excess pore water dissipation in the field.

In the present paper, the interactive behavior of the Pleistocene reclaimed foundations due to the construction of the adjacent reclamation of KIX is investigated based on the elasto-viscoplastic finite element analyses. Here, the mechanism for the propagation of excess pore water pressure in the Pleistocene deposits due to the adjacent construction is highlighted. The mass permeability of the Pleistocene sand gravel deposits is selected as one of the parameters controlling the deformation of the foundation ground. From those findings on the performance of excess pore water pressure, the mode of advance in settlement of the Pleistocene deposits is also discussed. The calculated performance is validated by comparing with the measured results. Based on the trial calculation, the authors show how to assess the actual behavior of the foundation ground that is taking place in the case of large-scale offshore reclamation such as KIX.

2. Framework of numerical assessment

2.1 Elasto-viscoplastic model

The elasto-viscoplastic constitutive model used in this paper was proposed by Sekiguchi (1977). Sekiguchi (1982) et al. modified the model to a plane-strain version. The viscoplastic flow rule for the model is generally expressed as follows:

$$\dot{\varepsilon}_{ij}^{p} = \Lambda \frac{\partial F}{\partial \sigma_{ij}^{'}} \tag{1}$$

in which F is the viscoplastic potential and Λ is the proportional constant. Viscoplastic potential F is defined as follows:

$$F = \alpha \cdot \ln\left[1 + \frac{\dot{v}_0 \cdot t}{\alpha} \exp\left(\frac{f}{\alpha}\right)\right] = v^{p} \tag{2}$$

in which α is a secondary compression index, $\dot{v}_o$ is the reference volumetric strain rate, f is the function in terms of the effective stress and vp is the viscoplastic volumetric strain. The concrete form of the model is shown in the reference (Mimura and Sekiguchi, 1986). The resulting constitutive relations are implemented into the finite element analysis procedure through the following incremental form:

$$\{\Delta\sigma^{'}\} = [C^{ep}]\{\Delta\varepsilon\} - \{\Delta\sigma^{R}\} \tag{3}$$

Where $\{\Delta\sigma^{'}\}$ and $\{\Delta\varepsilon\}$ are the associated sets of the effective stress increments and the strain increments respectively, and $[C^{ep}]$ stands for the elasto-viscoplastic coefficient matrix. The term $\{\sigma^{R}\}$ represents a set of 'relaxation stress', which increases with time when the strain is held constant. The pore water flow is assumed to obey isotropic Darcy's law. In relation to this, it is further assumed that the coefficient of permeability, k, depends on the void ratio, e, in the following form:

$$k = k_0 \cdot \exp\left(\frac{e - e_0}{\lambda_k}\right) \tag{4}$$

in which k_0 is the initial value of k at $e=e_0$ and λ_k is a material constant governing the rate of change in

permeability subjected to a change in the void ratio. Note that each quadrilateral element consists of four constant strain triangles and the nodal displacement increments and the element pore water pressure is taken as the primary unknowns of the problem. The finite element equations governing those unknowns are established on the basis of Biot's formulation (Christian, 1968, Akai and Tamura, 1976) and are solved numerically by using the semi-band method of Gaussian elimination.

2.2 Foundation model and hydraulic boundary

A series of elasto-viscoplastic finite element analyses is performed to assess the long-term settlement and the generation/dissipation/ propagation process of excess pore water pressure for the Pleistocene foundation of the 1st phase island due to the construction of the adjacent 2nd phase island of KIX. Figure 1 shows the plan view of the 1st and 2nd phase islands of KIX together with the location of monitoring point 1, where the differential settlement of the individual Pleistocene clay layers as well as the excess pore water pressure at various depth both in the clay and the sand gravel layers have been measured. A series of elasto-viscoplastic finite element analyses is carried out along the section shown by A-A' in Fig. 1. The model foundation used is schematically shown in Fig. 2 and the construction sequence is shown in

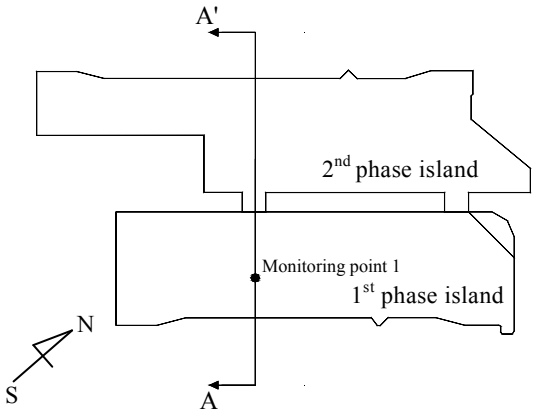

Fig. 1 Plan view of KIX (1st and 2nd phase) and the location of the monitoring point

Fig. 3 with the increasing process of the applied stress due to reclamation for two airport fills. It is necessary that the construction sequence for the airport fill is precisely modeled to better simulate the field. Figure 4 shows the reclaimed stress measured at center of the foundation of the 1st and 2nd phase islands respectively. The prescribed final overburden due to airport fill construction amounts to about 430kPa at the 1st phase island and about 530kPa at the 2nd phase island respectively. The 2nd phase reclamation is started after about 13years from the 1st reclamation. In Fig. 2, the model foundation used is assumed to be horizontally even layer having a constant thickness and continuous layer based on the boring data at the monitoring point 1. Here, Ma and Ds denote marine clay and Pleistocene sand gravel layer respectively, and the

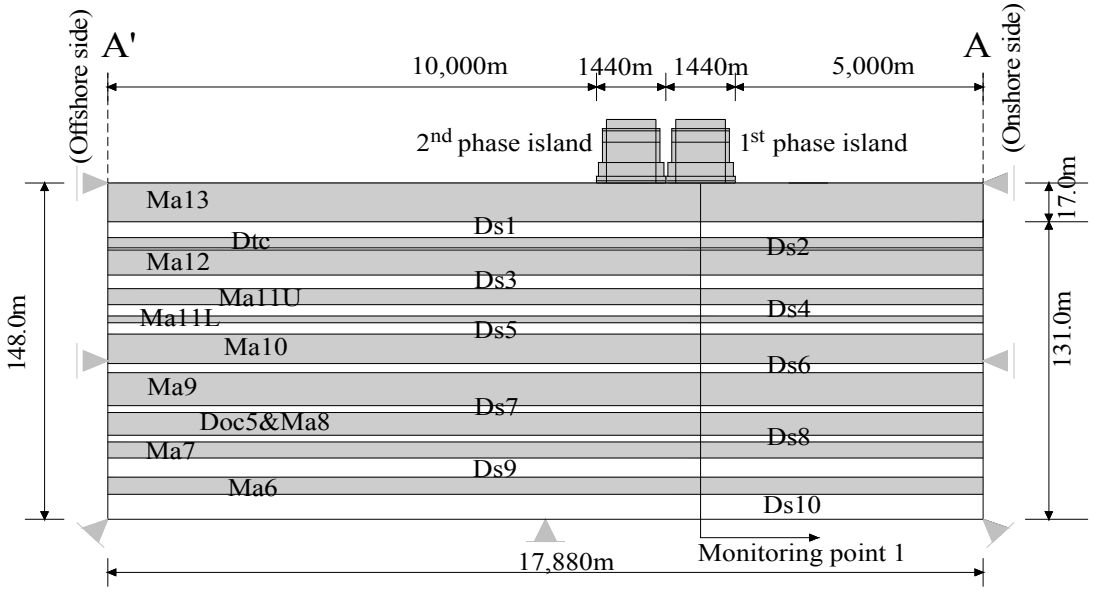

Fig. 2 Schematic cross-section of the foundation ground of KIX for finite element analysis

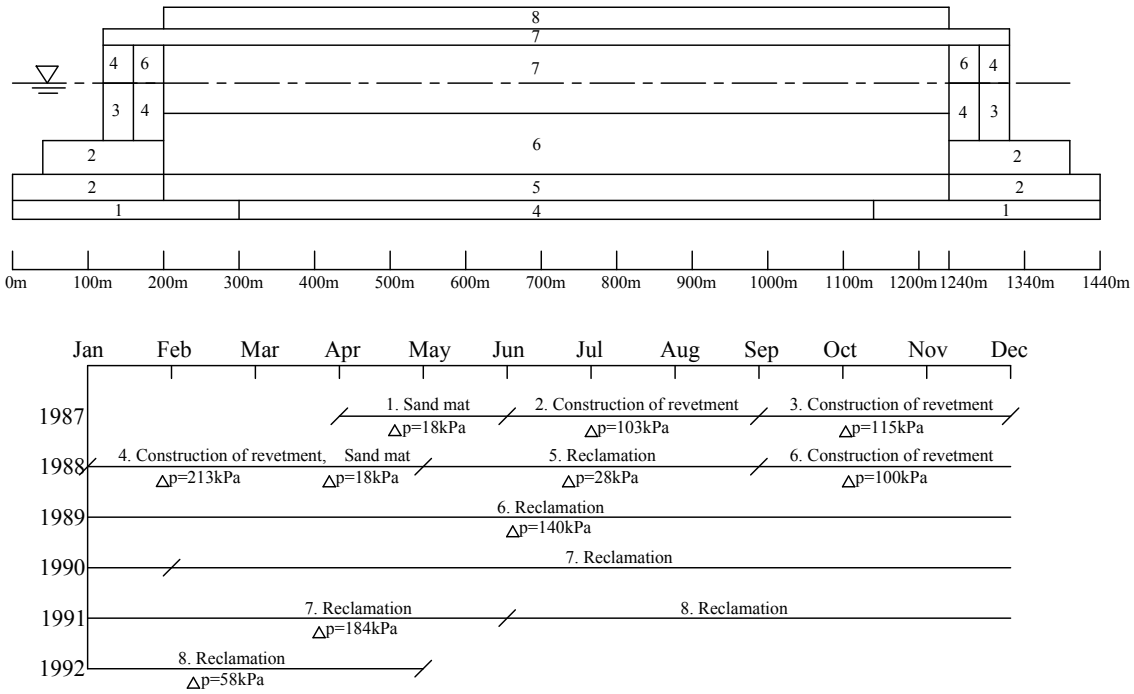

Fig. 3(a) Schematic cross-section of the airport fill and the construction sequence for the 1st phase island

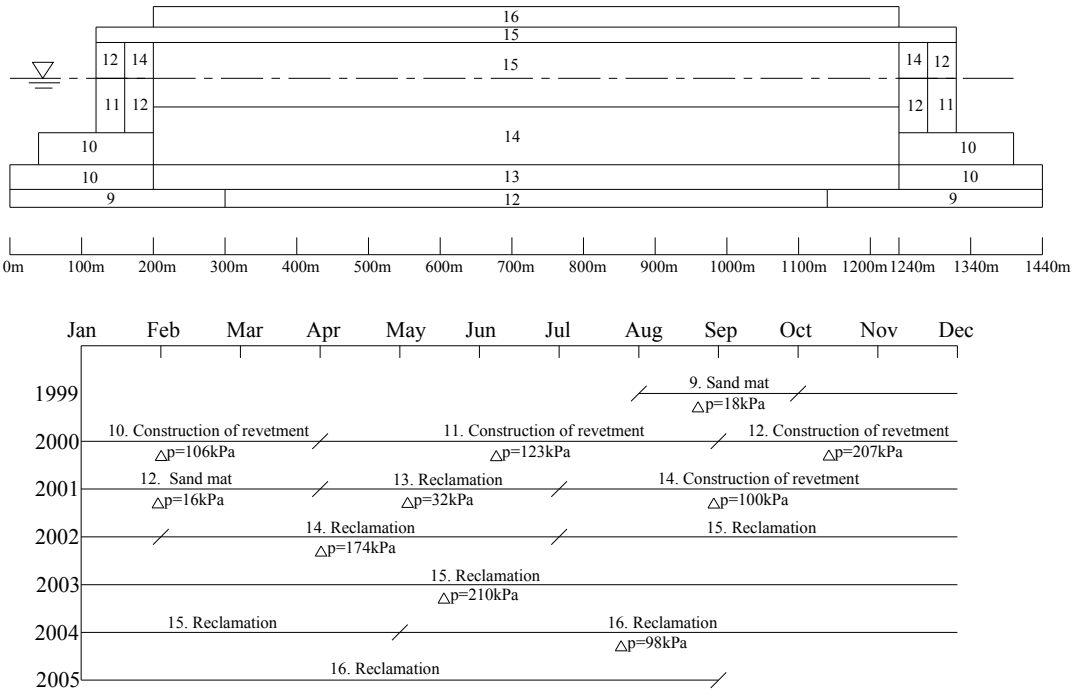

Fig. 3(b) Schematic cross-section of the airport fill and the construction sequence for the 2nd phase island

individual names of the Pleistocene clay layers have been updated to the present ones based on the geological findings from the boring KIX18-1 (Kitada et al., 2009). Ma13 is the Holocene marine clay whereas others are the Pleistocene origin. The original foundation is set from the elevation of -18m to -166m. For the normally consolidated Holocene clay deposit, Ma13, sand drains are driven in a rectangular configuration with a pitch of 2.0 to 2.5 meters to promote the consolidation. The

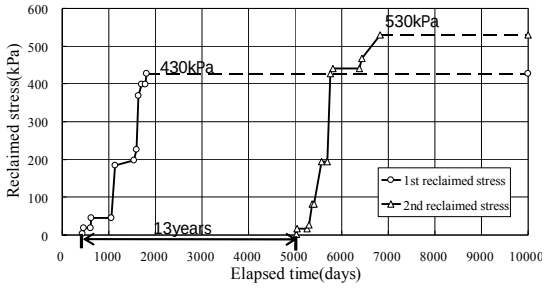

Fig. 4 Reclaimed stress with time for the 1st and 2nd phase reclamations

modeling of sand drains is simulated by the macro-element method (Sekiguchi et al., 1986). The lateral boundary of the clay layers (A-A' lines) in Fig. 2 is assumed to be undrained while that of the sand gravel layers is assumed to be fully drained. The bottom boundary is hence assumed to be undrained because Ds10 is underlain by Ma3 whose permeability is low enough to be impermeable. The hydraulic boundary condition on the sea side is influential for the subsequent deformation. In particular, the permeable sand gravel layers play a significant role to control the rate of consolidation (Mimura and Sumikura, 2000). It is natural that the calculated results are seriously influenced by the setting of boundary conditions. In the case of KIX, as there are alternating permeable sand gravel layers sandwiched by the Pleistocene clay layers, the propagation of excess pore water pressure through those permeable sand gravel layers should be of concern. Then, the effect of the mesh size in terms of the distance to the seaside boundary merits a due consideration on the subsequent deformation.

Mimura and Jang (2005) reported that when the distance to the boundary is set to be about 10 times of the loading area, the effect of the hydraulic boundary condition can be ruled out. Based on the findings, the FE mesh used in the present study is shown in Fig. 2. As shown in Fig. 2, while the loading area by reclamation of the 1st and 2nd phase island is 1,440m respectively, the distance to the right boundary is set to be 5,000m that is a distance from land in practice. For the opposite offshore side boundary, it is set to be 10,000m to make the numerical results be free from the effect of the hydraulic boundary.

2.3 Soil parameters

The Pleistocene clays in Osaka Bay exhibit slight overconsolidation due to the effect of diagenesis such as aging effect and/or development of cementation among clay particles. In this present analysis, the Pleistocene clay layers are assumed to be lightly overconsolidated, and the values of OCR are assumed to about 1.2 to 1.6 based on the result derived from conventional step loading

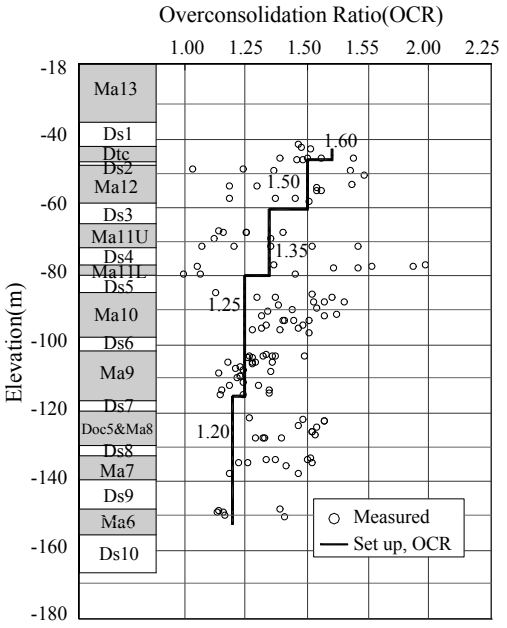

Fig. 5 Set up Overconsolidation Raito (OCR) for the Pleistocene clays

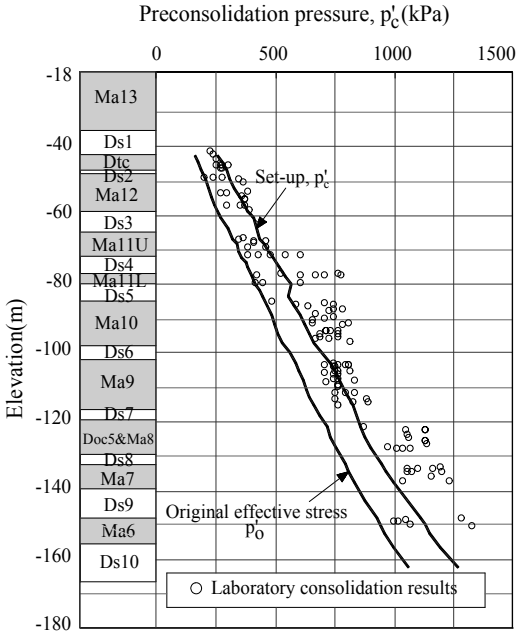

Fig. 6 Distribution of preconsolidation pressure (pc) with depth

consolidation test. Figure 5 shows the distribution of OCR with depth at the 1st phase island. The values of Pc below the Pleistocene clay Dtc layer is shown in Fig. 6. The Pleistocene sand gravel layers, which are expressed by Ds, are also assumed to be linear elastic material.

The model foundation for finite element analysis shown in Fig.2 is assumed to be horizontally continuous for the sand gravel layers sandwiched by the Pleistocene clay layers. But it was not definitely confirmed how the sand gravel layers under the Pleistocene marine foundation are distributed in practice. A due attention should be paid to the fact that the thickness, the horizontal continuity and the fine contents for the sand gravel layers are the influential factors to control the process of generation and dissipation of excess pore water pressure in the Pleistocene deposits. In present study, the concept of "mass permeability" is introduced. It is true that the values of the coefficient of permeability, *k* were derived based on the experiments but for such a large scale reclamation, those experimental values are meaningful as far as the distributed structure of the sand gravel layers are rationally modeled over a wide range. At present, the detailed distribution model for them cannot be established. Furthermore, the permeability controlling the advance in consolidation is not the one derived in the laboratory but the one that actually functions in the field. The authors consider this practical permeability as "mass permeability" that effectively controls the process of excess pore water dissipation in the field. The "equivalent coefficient of permeability" is hence introduced as a representative of "mass permeability" by considering the horizontal continuity, the change of thickness horizontally and the degree of fine contents for the Pleistocene sand gravel deposits. For convenience, the sand gravel layers are assumed to be level and continuous and the equivalent coefficients of permeability are provided for the individual sand gravel layers following the above-mentioned judgment. On the basis of the findings by Ito et al. (2001), the relatively high equivalent coefficients of permeability are assumed for Ds1, 3, 10 because they have been evaluated as gravelly, horizontally continuous and having enough thickness. On the other hand, very low equivalent coefficients of permeability are assumed for Ds 6 and 7 that have been evaluated to have insufficient thickness with high degree of fine contents and poorly continuous. The net values of the coefficient of permeability are applied to the rest sand gravel layers as "equivalent coefficient of permeability" because they have been evaluated as the ordinary permeable layers. The other soil parameters for the constitutive model are rationally determined based on the prescribed determination methods (Mimura et al., 1990, Mimura and Jang, 2004). The values of the principal soil parameters both for the Pleistocene clays and sand gravel layers are summarized in Table 1.

3. Results and discussions

3.1 Performance of excess pore water pressure

The calculated distribution of excess pore water pressure is shown in Fig. 7. As shown in Fig. 7(a), at the completion of the 1st reclamation (1800 days from the start of reclamation), little amount of excess pore water pressure remains in the Holocene clay layer because of the effect of sand drains. In contrast, a large amount of excess pore water pressure remains not only in the clay layers but also in the permeable sand gravel layers in the Pleistocene deposits. In particular, more than 200 kPa of excess pore water pressure is kept in the middle Pleistocene clay layers, Ma10 and Ma9 as well as sand gravel layers, Ds6 and Ds7. It should also be noted that excess pore water pressure propagates through the sand gravel layers outward from the loaded area even at the completion of reclamation. Remarkable decrease in effective stress hence takes place in the foundation where there is no reclamation load at the time. Here, a due attention should be paid to the fact that a slight propagation of excess pore water pressure takes place in Ds6 and Ds7 because the very low permeability of these sand gravel layers functions to obstruct sufficient propagation of excess pore water pressure. On the contrary, in the upper and lower Pleistocene deposits where the permeability of sand gravel layers is better than Ds6 and Ds7, serious propagation of excess pore water pressure can be seen. Propagation of excess pore water

Table.1 Principle soil parameters for the foundation of Kansai International Airport

MTYP	Quasi-OC region				NC region				M	ν'	K_0	p_0 (kPa)	p_c (kPa)	e_0	k_0 (m/day)	λ_k	Name of layers
	λ_{QOC}	κ_{QOC}	α_{QOC}	$\dot{v}_{0\,QOC}$ (day^{-1})	λ	κ	α_{NC}	$\dot{v}_{0\,NC}$ (day^{-1})									
1	0.0509	0.0051	6.06E-04	6.06E-07	0.5093	0.0509	6.06E-03	6.06E-06	1.40	0.35	0.540	4.0	19.1	3.20	8.64E-04	0.509	Ma13U-1
2	0.0532	0.0053	6.65E-04	6.65E-07	0.5321	0.0532	6.65E-03	6.65E-06	1.40	0.35	0.540	12.3	25.3	3.00	8.64E-04	0.532	Ma13U-2
3	0.0532	0.0053	6.99E-04	6.99E-07	0.5316	0.0532	6.99E-03	6.99E-06	1.40	0.35	0.540	20.8	31.6	2.80	8.64E-04	0.532	Ma13U-3
4	0.0518	0.0052	7.09E-04	7.09E-07	0.5178	0.0518	7.09E-03	7.09E-06	1.40	0.35	0.540	29.6	39.2	2.65	8.64E-04	0.518	Ma13U-4
5	0.0493	0.0049	7.14E-04	7.14E-07	0.4927	0.0493	7.14E-03	7.14E-06	1.40	0.35	0.540	38.9	47.9	2.45	8.64E-04	0.493	Ma13U-5
6	0.0510	0.0051	7.61E-04	7.61E-07	0.5097	0.0510	7.61E-03	7.61E-06	1.40	0.35	0.540	48.7	57.6	2.35	8.64E-04	0.510	Ma13U-6
7	0.0418	0.0042	6.86E-04	6.86E-07	0.4184	0.0418	6.86E-03	6.86E-06	1.40	0.35	0.540	57.7	66.9	2.05	8.64E-04	0.418	Ma13L-1
8	0.0489	0.0049	8.02E-04	8.02E-07	0.4889	0.0489	8.02E-03	8.02E-06	1.40	0.35	0.540	65.9	80.5	2.05	8.64E-04	0.489	Ma13L-2
9	0.0405	0.0040	6.98E-04	6.98E-07	0.4046	0.0405	6.98E-03	6.98E-06	1.40	0.35	0.540	76.2	91.7	1.90	8.64E-04	0.405	Ma13L-3
10	-	-	-	-	-	-	-	-	-	0.33	0.540	99.6	-	-	2.16E+01	-	Dsl -1
11	-	-	-	-	-	-	-	-	-	0.33	0.500	133.9	-	-	2.16E+01	-	Dsl -2
12	0.0239	0.0024	5.53E-04	4.12E-07	0.2392	0.0239	5.53E-03	4.12E-06	1.10	0.38	0.607	156.8	250.9	1.16	1.73E-04	0.239	Dtc-1
13	0.0218	0.0022	5.04E-04	3.76E-07	0.2182	0.0218	5.04E-03	3.76E-06	1.10	0.38	0.607	167.9	268.7	1.16	2.07E-04	0.218	Dtc-2
14	0.0341	0.0034	6.69E-04	4.99E-07	0.3406	0.0341	6.69E-03	4.99E-06	1.10	0.38	0.607	178.4	285.5	1.55	1.81E-04	0.341	Dtc-3
15	-	-	-	-	-	-	-	-	-	0.33	0.500	188.5	-	-	1.30E+00	-	Ds2
16	0.0684	0.0068	1.07E-03	1.75E-07	0.6840	0.0684	1.07E-02	1.75E-06	1.30	0.36	0.561	198.3	297.5	2.21	1.90E-04	0.684	Ma12U-1
17	0.0691	0.0069	1.11E-03	1.83E-07	0.6907	0.0691	1.11E-02	1.83E-06	1.30	0.36	0.561	208.3	312.5	2.10	1.47E-04	0.691	Ma12U-2
18	0.0600	0.0060	1.02E-03	1.68E-07	0.5997	0.0600	1.02E-02	1.68E-06	1.30	0.36	0.561	218.9	328.4	1.94	9.07E-05	0.600	Ma12U-3
19	0.0613	0.0061	1.11E-03	1.83E-07	0.6129	0.0613	1.11E-02	1.83E-06	1.30	0.36	0.561	230.3	345.4	1.76	9.50E-05	0.613	Ma12U-4
20	0.0499	0.0050	9.63E-04	1.58E-07	0.4985	0.0499	9.63E-03	1.58E-06	1.25	0.36	0.572	239.8	359.6	1.59	5.62E-05	0.499	Ma12L-1
21	0.0511	0.0051	9.87E-04	1.62E-07	0.5106	0.0511	9.87E-03	1.62E-06	1.25	0.36	0.572	246.9	370.4	1.59	5.62E-05	0.511	Ma12L-2
22	0.0523	0.0052	1.01E-03	1.66E-07	0.5227	0.0523	1.01E-02	1.66E-06	1.25	0.36	0.572	254.1	381.1	1.59	5.62E-05	0.523	Ma12L-3
23	-	-	-	-	-	-	-	-	-	0.33	0.500	284.1	-	-	1.08E+01	-	Ds3
24	0.0438	0.0044	8.90E-04	9.51E-07	0.4376	0.0438	8.90E-03	9.51E-06	1.20	0.37	0.583	315.4	425.8	1.46	9.50E-05	0.438	Ma11U-1
25	0.0460	0.0046	9.16E-04	9.79E-07	0.4605	0.0460	9.16E-03	9.79E-06	1.20	0.37	0.583	326.6	440.9	1.51	9.07E-05	0.460	Ma11U-2
26	0.0306	0.0031	6.80E-04	7.27E-07	0.3063	0.0306	6.80E-03	7.27E-06	1.20	0.37	0.583	340.0	459.0	1.25	7.08E-05	0.306	Ma11U-3
27	0.0102	0.0010	2.57E-04	2.75E-07	0.1024	0.0102	2.57E-03	2.75E-06	1.20	0.37	0.583	353.6	477.3	0.99	5.27E-05	0.102	Ma11U-4
28	-	-	-	-	-	-	-	-	-	0.33	0.500	384.6	-	-	3.89E+00	-	Ds4
29	0.0610	0.0061	1.20E-03	5.65E-06	0.6095	0.0610	1.20E-02	5.65E-05	1.25	0.36	0.572	412.3	556.6	1.54	5.88E-05	0.610	Ma11L-1
30	0.0311	0.0031	6.67E-04	3.15E-06	0.3105	0.0311	6.67E-03	3.15E-05	1.25	0.36	0.572	418.8	565.4	1.33	6.05E-05	0.311	Ma11L-2
31	0.0451	0.0045	9.83E-04	4.64E-06	0.4507	0.0451	9.83E-03	4.64E-05	1.25	0.36	0.572	425.8	574.8	1.29	6.48E-05	0.451	Ma11L-3
32	-	-	-	-	-	-	-	-	-	0.33	0.500	453.9	-	-	3.89E+00	-	Ds5
33	0.0393	0.0039	9.14E-04	2.55E-07	0.3935	0.0393	9.14E-03	2.55E-06	1.25	0.36	0.572	489.9	612.4	1.15	3.80E-05	0.393	Ma10-1
34	0.0518	0.0052	1.06E-03	2.97E-07	0.5177	0.0518	1.06E-02	2.97E-06	1.25	0.36	0.572	508.3	635.3	1.44	4.49E-05	0.518	Ma10-2
35	0.0578	0.0058	1.14E-03	3.17E-07	0.5779	0.0578	1.14E-02	3.17E-06	1.25	0.36	0.572	521.3	651.6	1.54	7.60E-05	0.578	Ma10-3
36	0.0754	0.0075	1.35E-03	3.76E-07	0.7538	0.0754	1.35E-02	3.76E-06	1.25	0.36	0.572	533.1	666.3	1.80	6.13E-05	0.754	Ma10-4
37	0.0786	0.0079	1.42E-03	3.97E-07	0.7859	0.0786	1.42E-02	3.97E-06	1.25	0.36	0.572	544.6	680.7	1.76	5.23E-05	0.786	Ma10-5
38	0.0562	0.0056	1.17E-03	3.27E-07	0.5621	0.0562	1.17E-02	3.27E-06	1.25	0.36	0.572	557.1	696.4	1.40	5.18E-05	0.562	Ma10-6
39	-	-	-	-	-	-	-	-	-	0.33	0.500	583.4	-	-	2.59E-01	-	Ds6
40	0.0563	0.0056	1.17E-03	3.18E-07	0.5625	0.0563	1.17E-02	3.18E-06	1.25	0.36	0.572	611.4	764.2	1.40	9.50E-05	0.563	Ma9-1
41	0.0638	0.0064	1.28E-03	3.48E-07	0.6383	0.0638	1.28E-02	3.48E-06	1.25	0.36	0.572	627.7	784.6	1.49	9.07E-05	0.638	Ma9-2
42	0.0722	0.0072	1.40E-03	3.79E-07	0.7216	0.0722	1.40E-02	3.79E-06	1.25	0.36	0.572	643.4	804.2	1.58	9.50E-05	0.722	Ma9-3
43	0.0765	0.0076	1.48E-03	4.02E-07	0.7646	0.0765	1.48E-02	4.02E-06	1.25	0.36	0.572	658.9	823.7	1.58	9.07E-05	0.765	Ma9-4
44	0.0659	0.0066	1.37E-03	3.71E-07	0.6591	0.0659	1.37E-02	3.71E-06	1.25	0.36	0.572	675.1	843.9	1.41	7.34E-05	0.659	Ma9-5
45	0.0512	0.0051	1.13E-03	3.07E-07	0.5125	0.0512	1.13E-02	3.07E-06	1.25	0.36	0.572	690.5	863.2	1.27	6.91E-05	0.512	Ma9-6
46	-	-	-	-	-	-	-	-	-	0.33	0.500	712.3	-	-	8.64E-02	-	Ds7
47	0.1590	0.0159	2.24E-03	1.58E-06	1.5904	0.1590	2.24E-02	1.58E-05	1.25	0.36	0.572	733.6	880.4	2.55	2.85E-05	1.590	Doc5&Ma8-1
48	0.0541	0.0054	1.11E-03	7.86E-07	0.5407	0.0541	1.11E-02	7.86E-06	1.25	0.36	0.572	750.3	900.3	1.43	7.78E-05	0.541	Doc5&Ma8-2
49	0.0368	0.0037	8.81E-04	6.23E-07	0.3678	0.0368	8.81E-03	6.23E-06	1.25	0.36	0.572	775.0	930.0	1.09	1.30E-05	0.368	Doc5&Ma8-3
50	-	-	-	-	-	-	-	-	-	0.33	0.500	804.4	-	-	2.16E+00	-	Ds8
51	0.0408	0.0041	9.41E-04	1.36E-06	0.4077	0.0408	9.41E-03	1.36E-05	1.25	0.36	0.572	828.3	994.0	1.17	1.30E-05	0.408	Ma7-1
52	0.0584	0.0058	1.16E-03	1.67E-06	0.5840	0.0584	1.16E-02	1.67E-05	1.25	0.36	0.572	845.5	1014.6	1.52	2.42E-05	0.584	Ma7-2
53	0.0343	0.0034	8.42E-04	1.22E-06	0.3430	0.0343	8.42E-03	1.22E-05	1.25	0.36	0.572	861.3	1033.6	1.04	3.02E-05	0.343	Ma7-3
54	-	-	-	-	-	-	-	-	-	0.33	0.500	910.9	-	-	2.16E+00	-	Ds9
55	0.0442	0.0044	9.91E-04	1.25E-06	0.4415	0.0442	9.91E-03	1.25E-05	1.25	0.36	0.572	961.4	1153.7	1.23	3.54E-05	0.442	Ma6-1
56	0.0387	0.0039	8.99E-04	1.13E-06	0.3869	0.0387	8.99E-03	1.13E-05	1.25	0.36	0.572	979.4	1175.3	1.15	4.49E-05	0.387	Ma6-2
57	0.0663	0.0066	1.49E-03	1.87E-06	0.6633	0.0663	1.49E-02	1.87E-05	1.25	0.36	0.572	997.4	1196.9	1.23	2.59E-05	0.663	Ma6-3
58	-	-	-	-	-	-	-	-	-	0.33	0.500	1035.9	-	-	6.92E+00	-	Ds10-1
59	-	-	-	-	-	-	-	-	-	0.33	0.500	1095.3	-	-	6.92E+00	-	Ds10-2

pressure in the Pleistocene sand gravel layers of the KIX foundations is associated with the insufficient dissipation of excess pore water pressure in them.

The phenomenon is caused by the insufficient capability of permeability of the Pleistocene sand gravel layers whose thickness is not enough for full dissipation of excess pore water pressure due to such huge reclamation load. In fact, almost full dissipation is achieved without significant propagation of excess pore water pressure both in Ds1 and Ds10 that have sufficient thickness and permeability. With the elapse of time, the excess pore water pressure in the upper Pleistocene clay layers such as Ma 12 and 11 monotonically dissipates whereas the one in the middle Pleistocene layers keeps unchanged (see Fig. 7 (b)). As is explained in the previous section, the low values of the coefficient of permeability are set for Ds6 and Ds7 because they are thin, poorly continuous and rich in fine contents. This low permeability of Ds6 and Ds7 causes the remarkable undissipated excess pore water pressure in those layers.

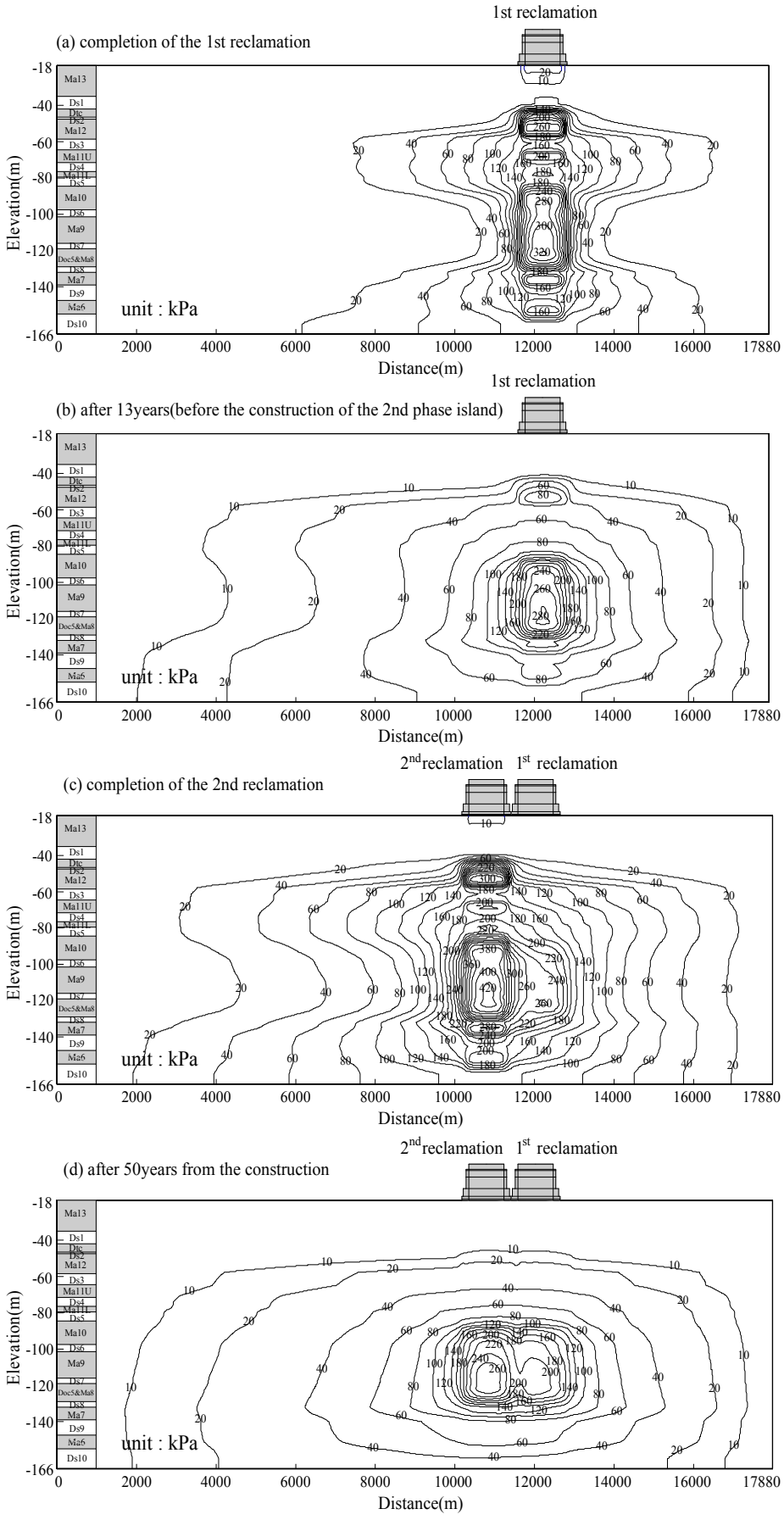

Fig. 7 Contours of the calculated distribution of excess pore water pressure

It is noteworthy in Fig. 7(b) that the excess pore water pressure in those layers is found not to dissipate even before the construction of the 2nd phase island (after 13 years since the start of reclamation). It clearly means that the primary consolidation in terms of the process of excess pore water pressure dissipation is not completed in the Pleistocene deposits before the construction of the 2nd phase island. Figure 7(c) shows the distribution of excess pore water pressure at the completion of the 2nd reclamation (after 19years since the start of the 1st reclamation). A large amount of excess pore water pressure also remains in the upper and middle Pleistocene clay layers, Ma12, 10, 9, and Doc5&Ma8 as well as sand gravel layers, Ds2, 6, and 7 below the foundation of the 2nd phase island. Here, a due attention should also be paid to the fact that the increased excess pore water pressure blow the foundation of the 2nd phase island is propagated to the one of the 1st phase island. As is explained above, the propagation of excess pore water pressure could be explained by the permeability of the Pleistocene sand gravel layers. Since the permeability of the upper and lower Pleistocene sand gravel layer is higher than the one of the middle layer, a larger amount of excess pore water pressure in the upper and lower Pleistocene layers is well propagated compared to the one of the middle layer in the foundation of the 1st phase island. As shown in Fig. 7 (b) and (c), it is found that more than 50kpa of excess pore water pressure in the upper and lower Pleistocene layer below foundation of the 1st phase island increases due to the construction of the 2nd phase island while the one in the middle Pleistocene layer is almost stable or slightly decreases. The low rate of excess pore water pressure propagation and dissipation is attributed to the poor permeability of sand gravel layers, Ds 6, 7. It is noteworthy that more than 200kPa of excess pore water pressure in those layers still remains undissipated even after 50years from the start of the reclamation (Fig. 7(d)). It clearly means that the primary consolidation in terms of the process of excess pore water pressure dissipation is not completed in the Pleistocene deposits for a very long time.

The distribution of the excess pore water pressure with depth at the monitoring point 1 that is located at the center of the 1st phase island (see Fig. 1,2) is shown in Fig. 8. The calculated values are compared with the measured one at three different times. Here, the solid line and ■, the chain dotted line and ◇, thin solid line and △ are the calculated and measured results at the completion of the reclamation of the 1st phase island , before the construction of the 2nd phase island and at the completion of the reclamation of the 2nd phase island respectively. Because the upper Pleistocene clays such as Ma12 and Ma11 have undergone plastic yielding due to reclaimed load, a large amount of excess pore water pressure generates at the completion of reclamation of the 1st phase island. Then it dissipates steadily because of the high permeability of the sand gravel layers, Ds1and Ds3 above and below Ma12. On the other hand, the mode of excess pore water pressure in the middle Pleistocene layers is different. Because of the poor quality of mass permeability of the sand gravel layers (Ds6, 7), Ma10, 9 and Doc5&Ma8 behave as if they were one continuous clay layer. Here, Ds6 and 7 does not seem to function as permeable layers at all. The rate of excess pore water pressure dissipation is very low in those layers, which results in that a large amount of undissipated excess pore water pressure remains in the middle Pleistocene

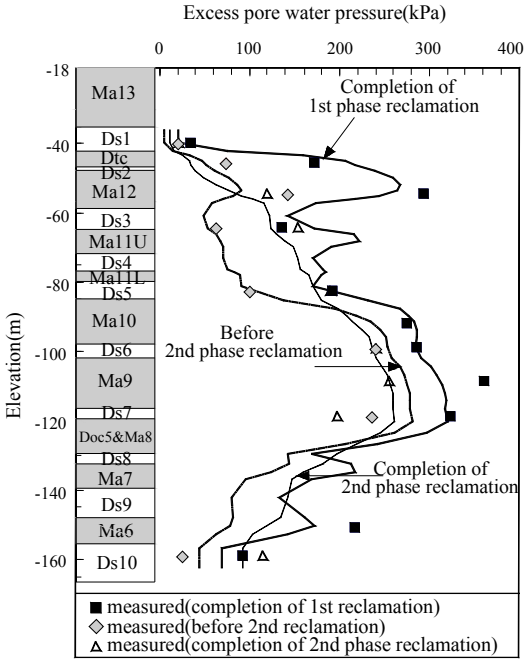

Fig. 8 Calculated and measured excess pore water pressure with depth at the monitoring point 1

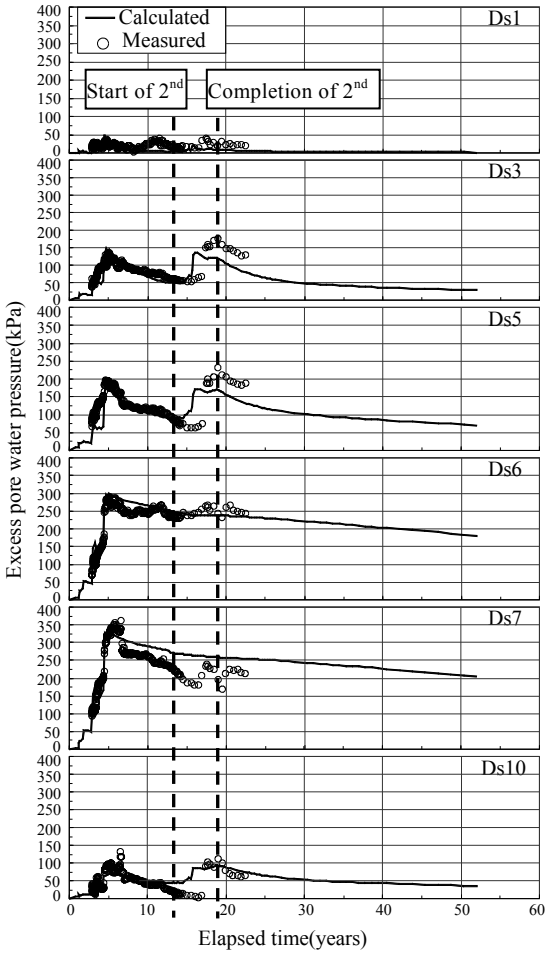

Fig. 9(a) Comparison of calculated and measured excess pore water pressure with time for the Pleistocene sand gravel layers

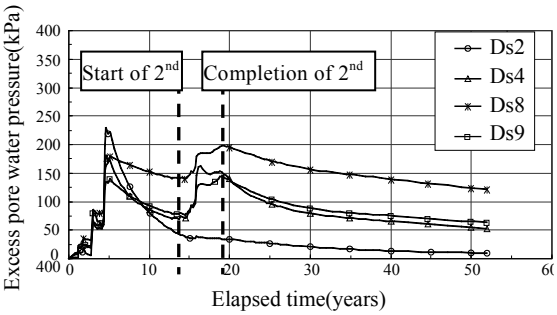

Fig. 9(b) Calculated performance of excess pore water pressure with time for the Pleistocene sand gravel layers

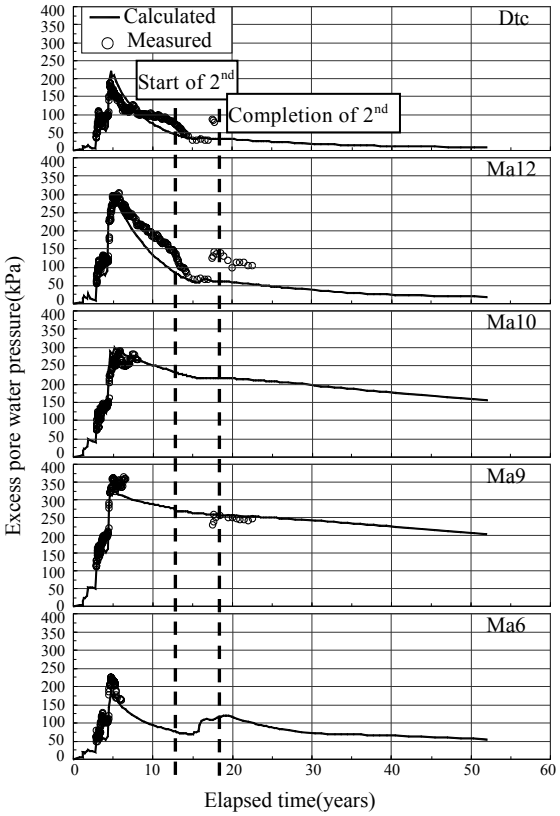

Fig. 9(c) Comparison of calculated and measured excess pore water pressure with time for the Pleistocene clay layers

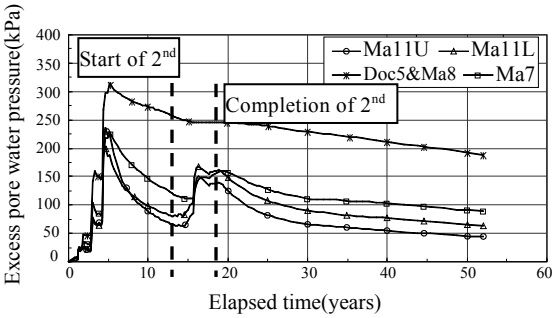

Fig. 9(d) Calculated performance of excess pore water pressure with time for the Pleistocene clay layers

layers for a long time. The calculated performance provides that even before the construction of the 2nd phase island, more than 200kPa of excess pore water pressure remains. In the lower Pleistocene layers such as Ma7, Ma6, the generated excess pore water pressure is not so large compared to the other layers and dissipates faster with time because of the high permeability of the thick sand gravel layer, Ds10 situated below Ma6. At the completion of the reclamation of the 2nd phase island, it is quantitatively found that the excess pore water pressure is propagated to the foundation of the 1st phase island due to the construction of the 2nd phase island. The excess pore water pressure increased remarkably due to the adjacent construction of the 2nd phase island in the upper and lower Pleistocene

layers because the sand gravel of those layers has an appropriate permeability as permeable layer. On the other hand, the one does not increase in middle Pleistocene layer such as Ma10, 9, Doc5&Ma8 and Ds6, 7 because the sand gravel layers, Ds6 and 7 does not function as well permeable.

Although the calculated performance at the completion of the reclamation of the 1st phase island slightly underestimates the measured excess pore water pressure at the layers such as Ma12, 9 and 6, the overall mode of distribution can be well described. In particular, the propagation of excess pore water pressure at the completion of the reclamation of the 2nd phase island can be well described. Therefore, long-term and interactive behavior of the excess pore water pressure in the Pleistocene deposits is found to be simulated with the present analyses.

Calculated excess pore water pressure - time relations are shown in Fig. 9(a) together with the measured results for the individual Pleistocene sand gravel layers. Note that the comparison is shown for the Pleistocene layers where the pore pressure cells have survived. It is clear that little excess pore water pressure is generated in Ds1 and Ds10 whereas large amount of excess pore water pressure is generated and kept undissipated in the middle Pleistocene sand gravel layers such as Ds6 and Ds7. The increase in excess pore water pressure due to the construction of the 2nd phase island is found in the upper and lower Pleistocene layers such as Ds 3, 5, 10. On the other hand, the excess pore water pressure is not well propagated in the middle of Pleistocene layers such as Ds 6, 7. Calculated performance can well predict the actual behavior of excess pore water pressure in the all Pleistocene sand gravel layers. Figure 9(b) shows the calculated performance of the excess pore water pressure of the Pleistocene sand gravel layers where they do not have the measured information due to damage of the pressure cells. The propagation of excess pore water pressure due to the construction of the 2nd phase island is shown in the Ds4, 8, 9. In Ds 2 layer, the excess pore water pressure is well dissipated without propagation because of high permeable layer, Ds 1 and the Holocene clay layer, Ma13 with sand drains. This difference remarkably reflects the mass permeability of the Pleistocene sand gravel layers. These behaviors of excess pore water pressure in the Pleistocene sand gravel layers are associated with the one in the Pleistocene clay layers. Calculated excess pore water pressure - time relations are shown in Fig. 9(c) together with the measured results for the individual Pleistocene clay layers. For the selected clay layers, the process of generation and dissipation of excess pore water pressure is well described by the present numerical procedure. Figure 9(d) shows the calculated performance of the excess pore water pressure of the Pleistocene clay layers where they do not have the measured information due to damage of the pressure cells. The process of excess pore water pressure propagation is similar to that of the Pleistocene sand gravel layers. It is also found that a rate of excess pore water pressure dissipation is very slow and the one is not propagated in the middle Pleistocene clay layers such as Ma10, 9. The phenomenon of undissipation in Ds6 and Ds7 causes the delay of consolidation for Ma10 and Ma9 associated with undissipation of excess pore water pressure. As seen from Figs. 9, the behavior of excess water pressure can be well predicted by the proposed procedure. It is hence confirmed that the adopted procedure in terms of elasto -viscoplastic finite element analysis associated with a new compression modeling and a concept of "mass permeability" works well to assess the stress condition of the reclaimed Pleistocene deposits at KIX.

3.2 Performance of effective stress

The consolidation behavior in the Pleistocene clay layer of KIX is dominated by change of the effective stress that is taken place by mechanism of generation/dissipation and propagation of excess pore water pressure due to the construction of the adjacent two islands. The stress condition with depth at the monitoring point 1 is shown in Fig. 10. Figure 10 also shows the stress condition at (a) the completion of the 1st phase reclamation, (b) before the 2nd phase reclamation, (c) the completion of the 2nd phase reclamation and (d) after 50years from construction respectively. Here, p_0 denotes the initial vertical effective stress, p_c is the consolidation yield stress, p_f means the final total vertical stress and p' denotes the effective vertical

stress due to the reclamation. The hatched area exhibits the undissipated excess pore water pressure. In Fig. 10(a), the effective stresses already surpass p_c for the Pleistocene clay layers above Ma10, while those still remain below p_c for the middle to lower Pleistocene clay layers such as Ma10, 9 and Doc5&Ma8. Then, the upper Pleistocene clay layers behave as normally consolidated and the middle to lower Pleistocene clay layers behave as overconsolidated at the completion of the reclamation of the 1st phase island. It is interesting that the stress condition of the airport foundations is not so different even before the start of the reclamation of the 2nd phase island as shown in Fig. 10(b). It is true that the excess pore water pressure at the upper Pleistocene layers is almost dissipated before the construction of the 2nd phase island, but the one at the middle Pleistocene clay layers scarcely dissipates during the period. A due attention should be also paid to the fact that the effective stress decreases in the upper and lower Pleistocene layers due to the construction of the adjacent 2nd phase island as shown in Fig. 10(c). On the other hand, in the middle Pleistocene layers, the effective stress does not decrease but rather increases slightly. The stress condition in the

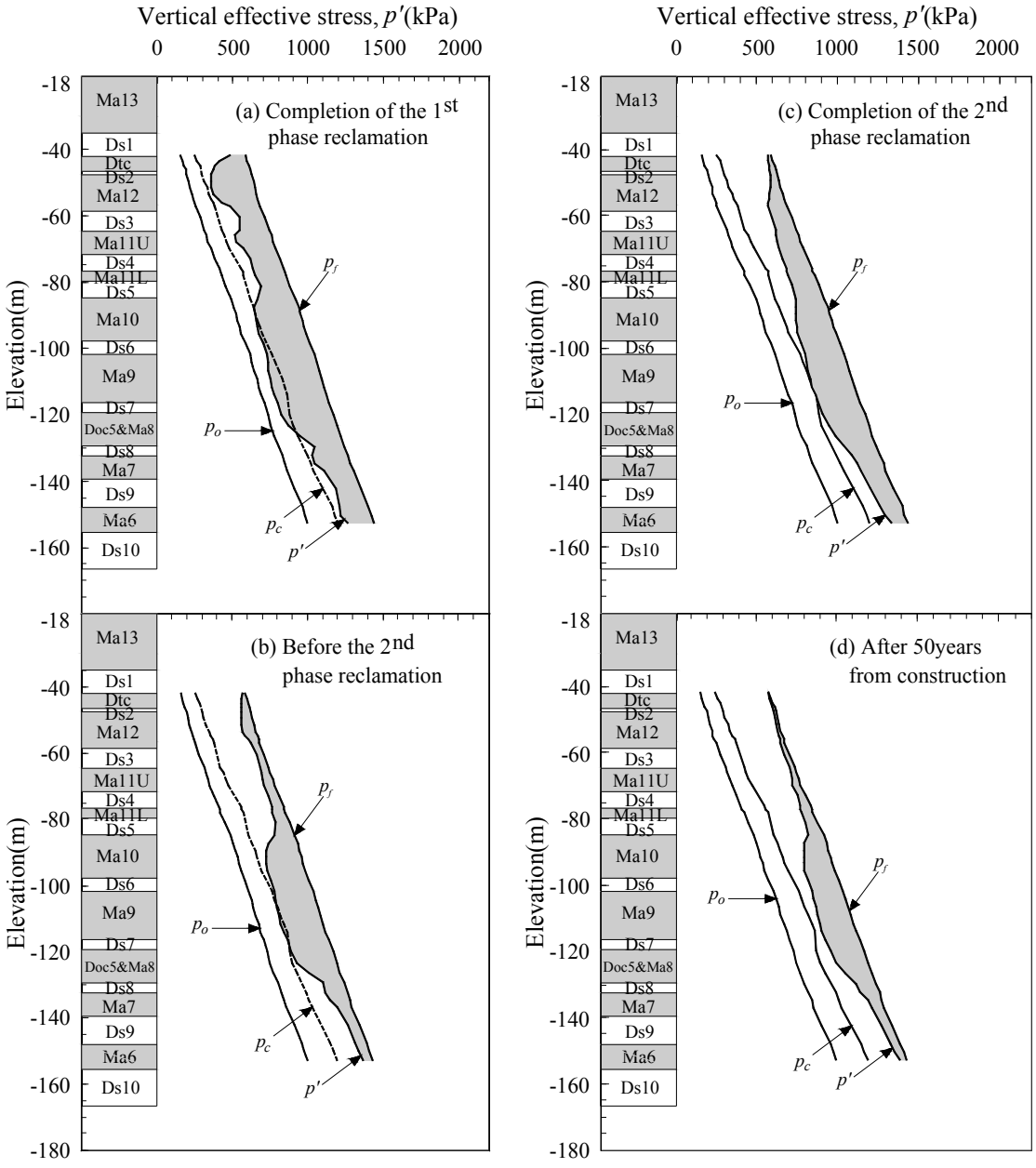

Fig. 10 Stress condition with depth at the monitoring point 1

middle Pleistocene layers is also not so different even at 50years from start of the project as shown in Fig. 10(d). One reason of this behavior is that the mass permeability of permeable sand gravel layers, such as Ds6 and 7 is insufficient to promote dissipation of excess pore water pressure and another is that the rate of consolidation for those layers becomes lower because the consolidation coefficients, c_v for Ma10 become much lower due to plastic yielding. From the results shown in Figs. 10, the advance in settlement due to consolidation for the middle Pleistocene clay layers is not greatly expected in this period.

3.3 Settlement

The calculated and measured settlement - time relations for the individual Pleistocene clay layers are shown in Fig. 11. As seen from Fig. 8, the excess pore water pressure in the upper and lower Pleistocene layers from Dtc to Ds5 and from Ma7 to Ds10 has steadily dissipated with time until before the construction of the 2nd phase island. This steady dissipation causes the remarkable advance in compression of those clay layers such as Dtc, Ma12, 11, 7 and 6. The compression of those clay layers is retarded or even slight expansion can be seen for some layers during the construction of the 2nd phase island because excess pore water pressure in the foundation of the 1st phase island increases due to propagation of excess pore water pressure from the foundation beneath the 2nd phase island. In the upper Pleistocene clay layers such as Dtc, Ma12 and 11, since after the completion of the 2nd phase reclamation, the primary consolidation with steady dissipation of excess pore water pressure is almost completed because of high permeability of sand gravel layers, Ds 1, 3 and 10. On the other hand, in the middle Pleistocene layers such as Ma10 to Ds7, the rate of dissipation of excess pore water pressure is much lower compared to the upper Pleistocene layers and excess pore water pressure does not increase during the construction of the 2nd phase island (see Fig. 9) because of the poor permeability of the sand gravel layers in this region. Although a rate of compression in those clay layers such as Ma10, 9 and Doc5&Ma8 is getting retarded due to the construction of the 2nd phase island, the process of compression is continues without remarkable

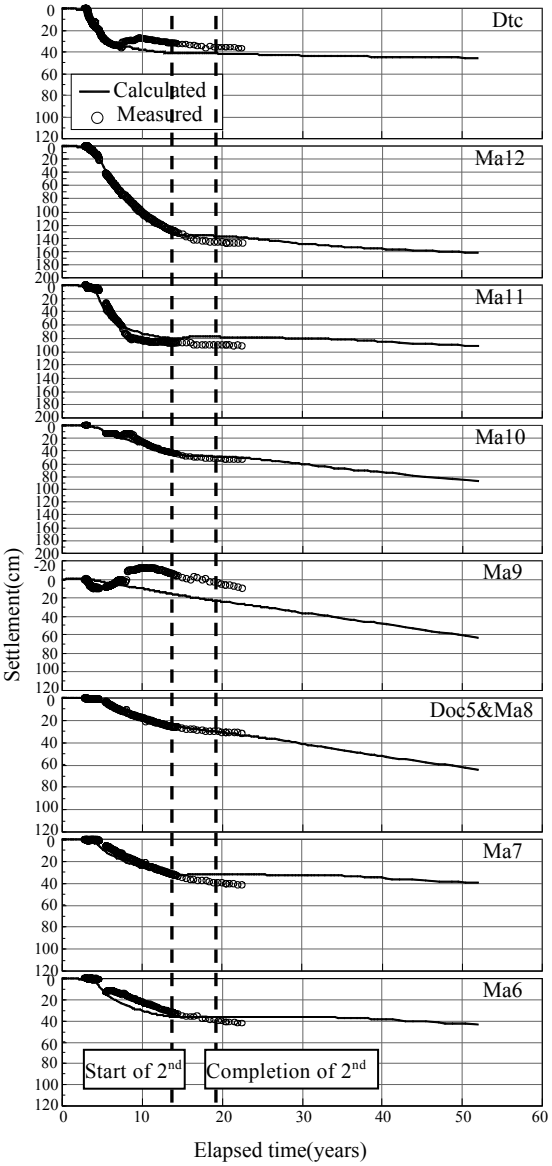

Fig. 11 Comparison of calculated and measured settlement with time for the Pleistocene clay layers at monitoring point 1

dissipation of excess pore water pressure. It means that the primary consolidation associated with dissipation of excess pore water pressure is not predominant in the middle Pleistocene clay layers. But the delayed compression including creep and secondary consolidation occurs during the process of excess pore water pressure dissipation under the condition of insufficient advance in primary consolidation. In all Pleistocene clay layers of KIX foundation ground, remarkable time dependent compression has hence continued without remarkable dissipation of excess pore water pressure. The comparison between the calculated

and measured settlement is also shown to confirm the validity of the proposed procedure in Fig. 11. In the upper Pleistocene clay layers such as Dtc, Ma12 and 11, the clays undergo plastic yielding due to reclamation load in a short time because of their relatively small initial stresses, p_o. Because the stress surpasses p_c so rapidly by the reclamation load, the time dependent behavior in the overconsolidated region can be ruled out and then as a typical behavior for normally consolidated clay, the hyperbolic shape for settlement – time relations is exhibited for Dtc, Ma12 and 11. The calculated performance can well describe the whole process of compression. On the contrary, in the middle Pleistocene clay layers such as Ma10, 9 and Doc5&Ma8, the stress remains within p_c at the completion of the reclamation of the 1st phase island. However, as shown in Fig 10, it takes a long time for these layers to become gradually normally consolidated by undergoing plastic yielding due to the dissipation of excess pore water pressure. During this process, the time dependent compression takes place with insufficient dissipation of excess pore water pressure. The calculated performance can also well describe the whole process of deformation.

In the lower Pleistocene clay layers such as Ma7 and 6, the mode of settlement with time is hyperbolic because of the sufficient permeability of Ds10. Different from the case for the middle Pleistocene clay layers, the dissipation of excess pore water pressure has advanced steadily with time. The calculated performance can well describe the measured settlement of Ma7 and 6.

4. Conclusions

The interactive behavior of the Pleistocene reclaimed foundations of the Kansai International Airport (KIX) due to the adjacent reclamation was numerically investigated. The elasto-viscoplastic finite element procedure is adopted by introducing the new assumption of non-elastic behavior in the quasi-overconsolidated region for the Pleistocene clays and the concept of mass permeability for the Pleistocene sand gravel layers. The original marine foundation was modeled with the assumption that the individual layers are horizontally even and continuous. The 1st phase island was constructed with 430 kPa of the reclaimed load followed by the construction of the 2nd phase island after 13 years with 530 kPa of the reclaimed load at 200m offshore of the 1st phase island.

It is natural that a large excess pore water pressure generated in the Pleistocene clay layers but the emphasis should be focused on the fact that even in the permeable Pleistocene sand gravel layers a large amount of excess pore water pressure was kept undissipated for a long time. Although the upper Pleistocene clay layers underwent the plastic yielding due to reclamation load in a short time, the excess pore water pressure dissipated steadily in these layers because of the existence of highly permeable sand gravel layers (Ds1and 3) in the vicinity. In contrast, the state of stresses of the middle Pleistocene clays remains in the quasi -overconsolidated region at the completion of the construction of the 1st phase island. Due to the insufficient dissipation of excess pore water pressure caused by the poor permeability of sand gravel layers in this region, it takes a long time for middle Pleistocene clays to become normally consolidated with dissipation of excess pore water pressure. The foundations of the 1st phase island were seriously affected by the reclamation of the 2nd phase island at 200m offshore from the 1st phase island. The most characteristic and influential phenomenon is “propagation of excess pore water pressure through the permeable sand gravel layers” in this particular case. Here, it should be noted that the Pleistocene sand gravel layers with poor permeability such as Ds 6 and 7 have been found not to function to propagate the excess pore water pressure generated due to the construction of the 2nd phase island to the foundation of the 1st phase island well because of their little permeability. On the contrary, the propagation of the excess pore water pressure is remarkable through the Pleistocene sand gravel layers with ordinary permeability such as Ds 3and 5. It is also found that excess pore water pressure could not propagate well through the Pleistocene sand gravel layers with very high permeability such as Ds 1 and 10 because of immediate dissipation in them as has been confirmed in the reclaimed foundations in Osaka Port. The calculated performance is found to well

describe the generation and dissipation process of the excess pore water pressure subjected to reclamation in the individual Pleistocene sand gravel layers of KIX.

Long-term compression of the Pleistocene clay layers have also been investigated with the present numerical procedure. Retardation and/or slight expansion were calculated for the Pleistocene clay layers due to the decrease in effective stress induced by the excess pore water pressure returned from the foundation beneath the 2nd phase island. Although the calculated performance slightly overestimates the heaving, it is found to describe the overall settlement over 20 years for the individual Pleistocene clay layers measured at monitoring point 1 in the 1st phase island.

Acknowledgements

The authors are grateful to Geo-research Institute for giving useful suggestions to determine the subsoil condition and the required parameters for finite element analysis.

References

Akai. K. and Sano, I. (1981): Long-term consolidation of Osaka upper diluvial clay, Tsuchi-To-Kiso, **29**(3), 43-47 (in Japanese).

Akai, K. and Tamura, T. (1976): An Application of Nonlinear Stress-strain Relations to Multi-dimensional Consolidation Problems. Annuals DPRI, Kyoto University, 21(B-2), pp.19-35 (in Japanese).

Christian, J.T.(1968): Undrained Stress Distribution By Numerical Method. Journal of Soil Mech. and Foundation Div., ASCE, 94 (SM6), pp.1333-1345.

Ito Y., Takemura, K., Kawabata, D., Tanaka, Y. and Nakaseko, K. (2001): Quaternary Tectonic Warping and Strata Formation in the Southern Osaka Basin Inferred from Reflection Seismic Interpretation and Borehole Sequences. Journal of Asian Earth Science, 20, pp.45-58.

Kitada, N., Takemura. K., Inoue, N., Ito, H., Masuda, F., Hayashida, A., Emura, T. and Fukuda, K. (2009): Stratigraphy of the drilling cores in Kansai International Airport (KIX18-1), Programme and Abstract, 39 Japan Association for Quaternary Research Meeting pp. 104-105 (in Japanese).

Kobayashi, G., Mitamura, M. and Yoshikawa, S. (2001): Lithofacies and sedimentation rate of Quaternary sediments from deep drilling cores in the Kobe area, Southwest Japan, *Earth Science*, **55**, 131-143 (in Japanese).

Mimura, M. and Jang, W.Y. (2004): Description of time-dependent behavior of quasi-overconsolidated Osaka Pleistocene clays using elasto-viscoplastic finite element analyses, Soils and Foundations, 44(4), pp. 41-52.

Mimura, M. and Jang, W.Y. (2005): Long-term Settlement of the Pleistocene Deposits due to Construction of KIA, proceedings of the Symposium on Geotechnical Aspects of Kansai International Airport, pp. 77-85.

Mimura, M. and Sekiguchi, H. (1986): Bearing Capacity and Plastic Flow of A Rate-sensitive Clay Under Strip Loading. Bulletin of DPRI, Kyoto University, 36(2), pp. 99-111.

Mimura, M., Shibata, T., Nozu, M. and Kitazawa, M. (1990): Deformation analysis of a reclaimed marine foundation subjected to land construction. Soils and Foundations, 30(4), pp. 119-133.

Mimura, M. and Sumikura, Y. (2000): Deformation and Excess Pore Water Pressure of the Pleistocene Marine Deposits due to Offshore Reclamation, Proc. Int. Symp. on Coastal Geotechnical Engineering in Practice, 1, pp.339-344.

Mimura, M., Takeda, K., Yamamoto, K., Fujiwara, T. and Jang, W.Y. (2003): Long-term settlement of the reclaimed quasi-overconsolidated Pleistocene clay deposits in Osaka Bay, Soils and Foundations, 43(6): 141-153.

Sekiguchi, H. (1977): Rheological Characteristics of Clays. Proc. 9th ICSMFE, 1, pp. 289-292.

Sekiguchi, H., Nishida, Y. and Kanai, F. (1982): A Plane-strain Viscoplastic Constitutive Model for Clay. Proc. 37th Natl. Conf., JSCE, pp. 181-182 (in Japanese).

Sekiguchi, H., Shibata, T., Fujimoto, A. and Yamaguchi, H. (1986): A Macro-element Approach to Analyzing the Plane-strain Behaviour of Soft Foundation with Vertical Drains. Proc. 31th Symp., JSSMFE, pp. 111-120 (in Japanese).

隣接海上埋立による更新統地盤挙動の相互作用に関する数値解析

田　炳坤*・三村　衛

*京都大学大学院工学研究科

要　旨

大阪湾泉州沖に海上埋立空港として建設された関西国際空港の基礎地盤は，更新統粘性土と砂礫層の互層構造を有しており，一期，二期空港島の建設によって大きな長期沈下を引き起こしている。各層ごとに測定されている過剰間隙水圧と圧縮量のデータから，透水層となるべき砂礫層内にも非常に大きな過剰間隙水圧が長期にわたって停留し，その一方で時間とともに沈下が続いていくという挙動を示している。本稿では，こうした更新統層の地盤挙動を弾粘塑性有限要素法によって解析し，層別の過剰間隙水圧と圧縮量の測定値と比較することにより，適用した解析手法の妥当性を検証する。その際，更新統粘土の擬似過圧密特性と砂礫層の“mass permeability”の概念を導入することが必要であることを明らかにする。これにより，一期，二期空港島の隣接埋立による関西国際空港基礎地盤の挙動を包括的に議論する。

キーワード:弾粘塑性有限要素解析，疑似過圧密，mass permeability，相互作用